Dual Pass Band Filter using Quad Stub Loaded Uniform Impedance Resonator

Anirban Neogi[1, 2], Jyoti Ranjan Panda[2]
[1]Supreme Knowledge Foundation Group of Institution,
Hooghly-712139, West Bengal, India
[2]School of Electronics Engineering
Kalinga Institute of Industrial Technology (Deemed to be University)
Bhubaneswar-751024, Odisha, India

Corresponding author: **Anirban Neogi** (e-mail: *anirbaan07.neogi@gmail.com*).

ABSTRACT A low loss, highly selective and miniaturized dual pass band filter for the wireless (WiMAX, WLAN) application is proposed in this paper. The filter is designed with Multimode Uniform Impedance Resonator (UIR) and multiple open stubs. The method of stepping down from a triple mode resonator to a dual mode resonator for better performance is presented. Two different coupling schemes (electric and magnetic) are observed for the said dual pass bands. A detail analysis about the dimension of the resonators, resonating conditions and frequency calculations are depicted in this paper. The dual pass bands are achieved at 3.45 GHz and 5.4 GHz with minimum pass band insertion loss (|IL|) 0.1 and 0.18 dB and the pass band Fractional Band widths (FBW) 4% and 8% respectively. With proper optimizations, Transmission Zeros (TZ) are achieved on both sides of the dual pass bands and the spurious pass band are kept around -20dB level and hence good selectivity is achieved. The overall size of the filter is optimized for the best possible results in terms of Insertion Loss, Return Loss and selectivity, is found to be (24.2 x 21) mm = (0.28 x 0.24)λ_g = 0.06 λ_g^2.

INDEX TERMS Dual Bandpass Filter, Admittance Ratio, Electrical Functional Circuit, Insertion Loss, External Quality Factor.

I. INTRODUCTION

MULTIBAND filters, especially the dual band filters have several applications in wireless communication. Research on dual band filters is boosted up in last two decades on the basis of low cost, high selectivity, excellent stop band performances and size miniaturization. Various methods, mathematical models and analytical tools were used to achieve these goals.

In [1, 2], the asymmetric transmission zero technique to develop dual pass band filter was described with excellent selectivity and good IL. But the overall size of the filter is an issue to discuss with. Two excellent proposals were found in [3, 4], where the first one employed UIR and hairpin resonator and the second one used electric and magnetic coupling scheme to develop dual pass band filters. But Apart from all the excellent characteristics both are seriously lagging in terms of Insertion Loss (IL). One hexagonal split ring resonator was used in [5], to design a dual pass band filter with size miniaturization and good IL, but seriously lagged behind from Return Loss point of view. A dual layer, dual mode resonator approach was taken in [6], to achieve controllable TZ and to improve the selectivity of the filter. Overall size of the filter is also appreciable. But again, the pass band IL is very poor. Similarly [7, 8] both lags from the IL point of view though they have excellent stop band characteristics. On the other hand, the proposed filter in [9] shows excellent pass band characteristics in terms of IL and RL but TZ is missing on the left side of first pass band and hence it degrades the selectivity. While analyzing [10, 11, 12] it is found that the Fractional BW of these filters is in the higher side though they give excellent performance in terms of overall size. One Quasi-planner resonator was introduced in [13], which showed excellent performance in terms of FBW and IL, but the size of the filter and absence of TZ will degrade the stop band performances. A substrate Integrated Waveguide (SIW) is well explained in [14], and to achieve the finest IL and FBW the overall size of the filter is again compromised. So, it is well observed that appreciable pass band and stop band performances and size miniaturization at the same time is very hard to achieve.

In this research, we have proposed one simple and compact dual pass band filter with excellent pass band and stop band performance. The filter is designed on Arlon AD 250 substrate of dielectric constant 2.5 and height 0.76 mm. The filter simulation is done with HFSS 13 which generates two pass bands at 3.45GHz and 5.4 GHz, with in band Insertion Loss |0.1| & |0.18| dB and with FBW 4% & 8% respectively. These pass bands are suitable for WiMAX and WLAN applications. The overall size of the filter is (24.2mm x 21mm) = 0.28 λ_g x 0.24λ_g = 0.06 λ_g^2, where λ_g is the guided wavelength at the center frequency of first pass band.

II. THE RESONATOR ANALYSIS

A. THE PROPOSED RESONATOR

A basic Quad mode Stub Loaded UIR (QMSLUIR) is shown in Figure1a), which generates four resonating modes in the specified frequency band of 0-8Ghz [15]. All the stubs are symmetrically and centrally loaded around the UIR structure. In this study, we have changed the orientation of the stub loading around the UIR structure such as four open stubs are placed along four corners of UIR structures as shown in Figure 1b). The side stubs are of length L_1 and the vertical stubs are of length L_3. The length of the UIR is $2L_2$. Once the structure of 1a) is converted in 1b), the quad mode resonator is converted into tri mode resonator and it produces lesser Insertion Loss compared to 1a). The dimensions of L_1, L and L_3 are kept same in Figure 1a) and 1b). The multipath coupling schemes (one through side stubs and another through vertical stubs) in the proposed resonator enable individual bandwidth control. Under weak coupling condition the frequency response of 1b) is shown in Figure 2.

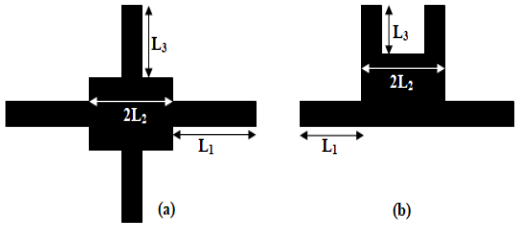

FIGURE 1. Basic resonator structure under weak coupling a) Quad Mode b) Tri Mode

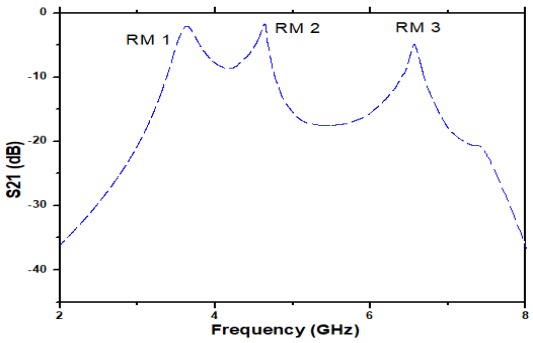

FIGURE 2. Frequency response of Tri Mode resonator

The study of the resonator depicted in Figure 1b) is very interesting in terms of its dimensions. It is well observed under different simulating conditions that, L_1 and L_3 are playing all important roles in deciding the resonating modes (RM). From Figure 3, while L_1 is changing from 7 to 13.5 mm (with L_3 = 9 mm), the first and second resonating modes shift from 4 to 3.2 GHz and 4.9 to 4.5 GHz respectively, whereas the third resonation mode remain constant at 6.58 GHz. Similarly, from Figure 4, it is observed that when L_3 changes from 6 to 9 mm (with L_1 = 11 mm), the third and second resonant frequencies are changing from 6.57 to 5.78 GHz and 4.65 to 5 Ghz respectively, whereas the first resonant mode remains constant at 3.62 GHz.

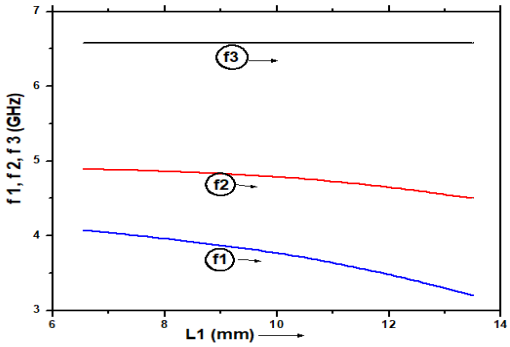

FIGURE 3. f_1, f_2, f_3 variation with L1

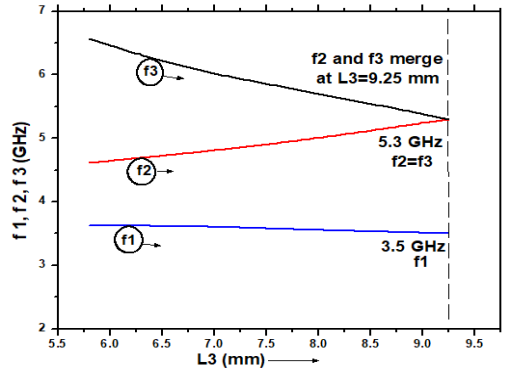

FIGURE 4. f_1, f_2, f_3 variation with L3

As per Figure 4 it may be well observed that, as the value of L_3 is increasing the second and third resonating modes are closing towards each other. At L_3=9.25 mm the second and third modes overlap with each other, and the tri mode resonator is converted into a dual mode resonator (Figure 5). The centre frequency of the overlapped resonating mode is 5.3 GHz. Therefore, the dual resonating modes are 3.5 and 5.3 GHz at L_1 = 11.5 mm and L_3 = 9.25 mm. The first resonating mode is determined by the UIR structure along with the side stubs, whereas the second resonating mode is determined by the UIR and vertical open stubs. The dependency of f_1, f_2 and f_3 on L_1 and L_3 are well explained through Figure 3 &4. It is clear that f_1 and f_3 can be solely controlled by L_1 and L_3 respectively. Meanwhile we can find the variation of f_2 with respect to L_1 and L_2 both. But it is also important to understand that the rate of change of f_2 is almost half compared to the f_1 and f_3 rate of variations. The effect of all the width of microstrip open stub lines on f_1, f_2 and f_3 are very nominal and hence can be ignored.

$$f_1 = f_{even1} = \frac{C}{(4L_1)\sqrt{\varepsilon_{eff}}} \quad (1)$$

$$f_3 = f_{even2} = \frac{C}{(4L_3)\sqrt{\varepsilon_{eff}}} \quad (2)$$

$$f_2 = f_{odd} = \frac{C}{2(L_1 - L_3)\sqrt{\varepsilon_{eff}}} \quad (3)$$

f_1 is found to be inversely proportional to L_1 and for the sake of numerical equilibrium, exactly to $4L_1$. Then with respect to the reference given [16], the final expression of equation (1) created. f_2 decreases with L_1 and increases with L_3. So it is inversely proportional to (L_1-L_3). The rate of

change of f_2 is numerically double compared to (L_1-L_3).

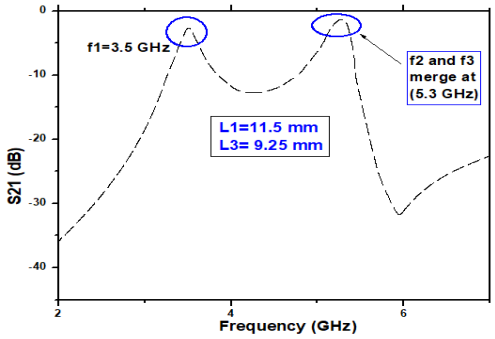

FIGURE 5. RM2 and RM3 merge at 5.3 GHz

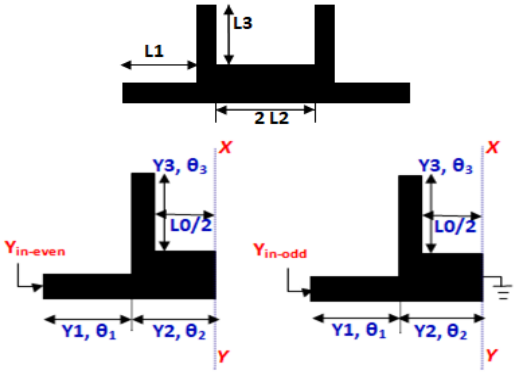

FIGURE 6. Even-Odd mode analysis of proposed resonator

Since the resonating structure proposed in Figure 1b) is symmetrical in nature, it may be realized by Even-Odd mode analysis. The Even and Odd mode equivalent circuits are shown in Figure 6. The dimensions marked with L, θ and Y represents the corresponding physical length, electrical length and admittance of the microstrip lines. Under Even mode excitation there is no current flow through the symmetrical plane X-Y. In the same way there should be null voltage in the X-Y plane under odd mode excitation. The Even mode generates two resonant frequencies f_{Even1}=f_1 and f_{Even2}=f_3. Whereas the Odd mode generates single resonant frequency f_{Odd} =f_2. From Even and Odd mode equivalent circuit of Figure 6, the resonant conditions of both the modes can be calculated in terms of input admittance [17]. Let us define the admittance ratio of the side stubs and vertical stubs with UIR structure as $K_1 = \frac{Y_1}{Y_2}, K_1 = \frac{Y_3}{Y_2}$.

For Odd Mode analysis

$$Y_{in-odd} = jY_1\left(\frac{Y_1 tan\theta_1 - Y_2 cot\theta_2 + Y_3 tan\theta_3}{Y_1 - Y_2 tan\theta_1 cot\theta_2 - Y_3 tan\theta_1 tan\theta_3}\right)$$

$$= jY_1\left(\frac{Y_1 tan\theta_1 tan\theta_2 - Y_2 + Y_3 tan\theta_3 tan\theta_2}{Y_1 tan\theta_2 - Y_2 tan\theta_1 - Y_3 tan\theta_1 tan\theta_2 tan\theta_3}\right) \quad (4)$$

At resonance Y_{in}= 0 and we find

$$Y_2 = Y_1 tan\theta_1 tan\theta_2 + Y_3 tan\theta_3 tan\theta_2$$

$$K_1 tan\theta_1 tan\theta_2 + K_2 tan\theta_3 tan\theta_2 = 1 \quad (5)$$

Similarly for Even mode

$$Y_{in-even} = jY_1\left(\frac{Y_1 tan\theta_1 + Y_2 tan\theta_2 + Y_3 tan\theta_3}{Y_1 - Y_1 tan\theta_1 tan\theta_2 - Y_3 tan\theta_1 tan\theta_3}\right) \quad (6)$$

At resonance $\mathbf{Y_{in}}$ = 0 and we find

$$K_1 tan\theta_1 + K_2 tan\theta_3 + tan\theta_2 = 0 \quad (7)$$

Equation (5) and (7) describe the resonance conditions under odd and even mode analysis respectively. With L_1 = 11.5 mm and L_3 = 9.25 mm, when the resonator structure of Figure 1b) acts as dual mode resonator, the center frequency of two resonating modes are 3.5 and 5.3 GHz. The resonator is built on a substrate of dielectric constant 2.5 with height 0.76mm. The admittance ratios can be readily calculated as K_1= 0.28 and K_1= 0.35.

B. THE FILTER DESIGN

The proposed layout of the dual band filter is shown in Figure 7. A pair of Quad Stub Loaded UIR (QSLUIR) are coupled together to form the desired filter. The open side stubs that are parallel coupled with extended (~) 50 ohm feed line, are responsible for generating the first pass band. The other two vertical open stubs from both the resonators are contributing to generate the second pass band. This is well explained through Figure 3 & 4, that the dependency of f_1 and f_3 are solely on L1 and L3 respectively. Also, we have adjusted L1, L2, and L3 in order to convert the tri mode resonators in dual mode resonators. Once f_2 and f_3 merges (beyond L3= 9.25 mm), the first and second pass bands can be controlled individually through L1 and L2 respectively. Therefore, we may conclude that, the first pass band is f_{Even1}=f_1 whereas the second pass band is corresponding to f_{Even2}=f_3= f_{Odd} =f_2. Dual pass bands center frequencies are found to be 3.45 and 5.4 GHz. To minimize the size of the filter the open stubs are folded back to form spiral or meander like structure. The vertical open stubs from UIR structure is bended in such a way that they become side coupled. The coupling gap (d1) between them is another powerful parameter to adjust the second band center frequency.

The filter functionality may be explained again by its simplified functional circuit [18] as shown in Figure 8. L_p and C_p represents the effective equivalent inductance and capacitance of I/p and o/p feed lines. C_c is the equivalent coupling capacitance between feed line and side stubs of the UIR. As stated earlier, C_d is the gap capacitance (gap d1) between the vertical and folded open stubs. As indicated in Figure 8, path1 is determining the center frequency of first pass band and path 2 is creating the center frequency of second pass band. The path 1 is coupled through electric coupling, whereas magnetic coupling is there in path 2. Considering both the resonators from Figure 7, the mixed coupling factor can be approximated as [17]

$$K = \frac{f_2^2 - f_1^2}{f_2^2 + f_1^2} \quad (8)$$

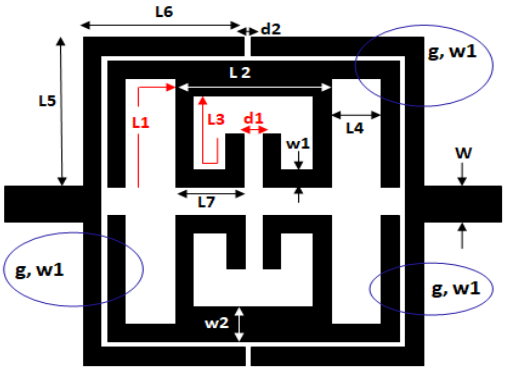

FIGURE 7. Layout of the proposed Dual band BPF

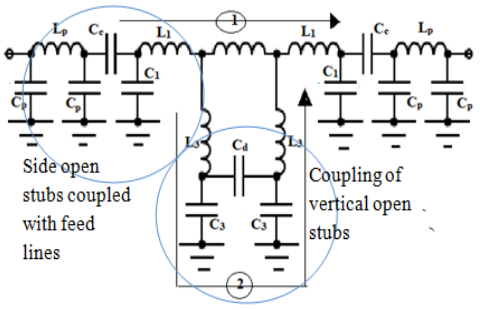

FIGURE 8. Functional circuit of proposed Dual BPF

The frequency response of the proposed filter is shown in Figure 9. Clearly the dual pass bands center frequencies are 3.45 and 5.4 GHz. L1, L3 and d1 are finitely optimized to achieve the smooth dual pass bands. It is already well explained through Figure 3 & 4 that L1 optimization will give us 1st pass band whereas L3 optimization will be responsible for second pass band. The vertical stub coupling gap d1 creates Transmission Zero (TZ) on both side of second pass band. Another TZ on the left of first pass band is realized by extending the length of outer feed line (L5+L6). The spurious pass bands on both sides of the 1st and 2nd pass bands are kept in -20dB region. The microstrip line width (W1) and the gap (g) between two parallel strip lines are kept same throughout the layout. It is already mentioned that the multiple coupling schemes (one through side stubs and another through vertical stubs) in the proposed resonator enable individual pass band characteristics control. For the first pass band, if we consider the side stub L1, proper optimization of its length and width will create nearest possible impedance matching with i/p – o/p feed line. In addition, the optimization of L2 and W2 will also regulate the characteristic impedance of the UIR section. For the second pass band optimization of L3 and d1 will create minimum IL by properly choosing K and Qe [19, 20]. The overall size of the proposed filter is (24.2mm x 21mm) = 0.28 λ_g x 0.24λ_g = 0.06 λ_g^2. The parametric values of the proposed layout with respect to Figure 9 are as follows (in mm), L1 = 8.4, L2 = 12, L3 = 9.55, L4 = 2.5, L5 = 6.8, L6 = 9.4, L7 = 5.7, W = 2.2, W1 = 0.5, W2 = 2.75, d1 = 0.59, d2 = 1, g = 0.5.

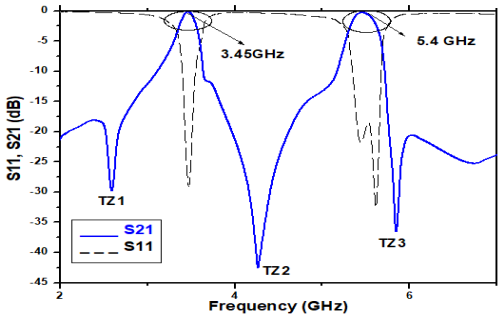

FIGURE 9. Frequency Response of Proposed dual Band Filter

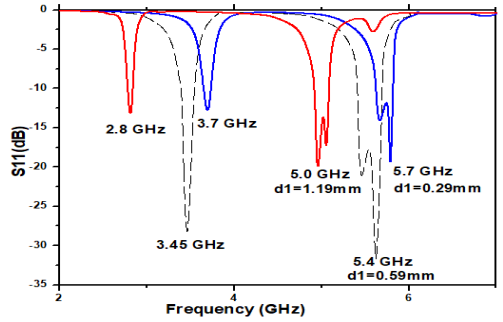

FIGURE 10. Parametric Study with d1

III. MEASURMENT AND RESULT ANALYSIS

A. PARAMETRIC STUDY

The frequency response of the proposed filter is presented through Figure 9. Apart from its dual band performance the response shows three Transmission Zeros at 2.6, 4.26 and 5.82 GHz. The simulation shows excellent results in terms of Insertion Loss (IL) and Return Loss (RL). We find |IL|=0.10 dB, |RL|= 29dB at 3.45 GHz and at 5.4GHz the values are |IL|=0.18 dB, |RL|= 32 dB. The S_{11} (dB) graph exhibits a sharp glitch at second pass band which is indicative of the overlapping of two resonating mode. The importance of vertical open stub coupling is already discussed in previous section. The degree of this coupling is controlled by d1. The parametric study of d1 is presented in Figure 10. The change in d1 will affect the admittance ratio of both the resonators and hence the resonant frequencies. Thereafter from (8), different values of K can be calculated for d1 variations. At d1=0.59mm we get the desired response with K=0.45.

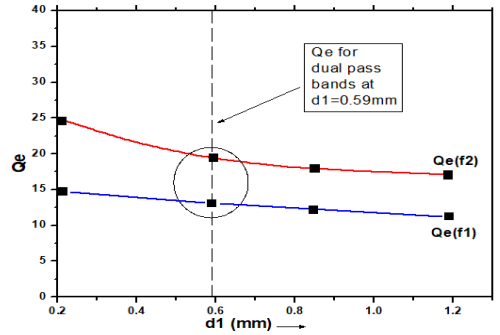

FIGURE 11. Q_e of the proposed filter with d1

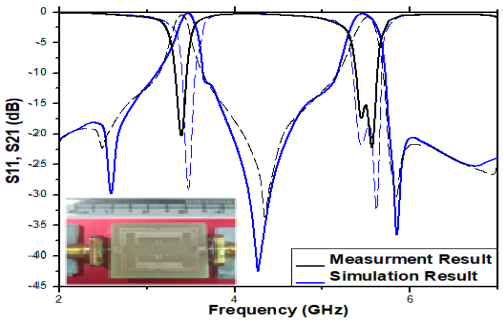

FIGURE 12. Fabricated prototype and comparison of Simulated and measured frequency responses

From Figure 9 we can calculate the Fractional Bandwidth (FBW) of the dual pass bands. When the value of d1 varies, center frequencies of both the pass bands changes and hence the FBW. When d1=0.59mm, the new pair of dual pass band center frequencies will be generated (Figure 10), which will have different FBW. The External Quality factor (Q_e) may be defined as [21]

$$Q_e = \frac{g_0 g_1}{FBW} = \frac{w_0}{3dB\ (abs)BW} \quad (9)$$

Where w_0 is the centre frequency and *(abs) BW* stands for absolute 3dB bandwidth. The element values of corresponding low pass prototype are found to be g_0=1, g_1=0,998. So, either by theoretical calculations or by HFSS simulations Q_e can be calculated for different values of d1. The variation of Qe with d1 is presented in Figure 11.

B. MEASUREMENT RESULT

To support the validity of our simulation, fabrication of proposed prototype is done and |S11| & |S21| parameters are measured. The measured results almost followed the simulation and hence validate the simulation as shown in Figure 12. The center pass band frequency of first and second bands shifted little bit to 3.40 and 5.35 GHz respectively. The Pass band Insertion Loss degraded to |0.22| and |0.3| dB from |0.10| and|0.18| dB respectively for first and second pass band. All the transmission zeros are available in measured result and the harmonic pass bands are still around -20dB level, which suggests the excellence of fabrication. The overall dimension of the prototype is (24.2mm x 21mm) = 0.28 λ_g x 0.24λ_g = 0.06 λ_g^2 (Figure 12). The proposed dual band filter is compared with some of the contemporary research articles as shown in Table-1.

Table 1. Comparison of proposed filter with other contemporary works

Ref.	*Dual band Centre Freq. (GHz)*	*Min.IL (dB)*	*RL (dB)*	*FBW (%)*	*Size (λ_gxλ_g)*
[5]	2.54, 4.85	0.45,0.6	12,20	18,8	0.28x0.26
[12]	1.17,4.06	0.48,0.87	35,25	82.5,20.6	0.12x0.14
[22]	2.4,5.2	0.82,1.17	10,10	17.3,14	0.32x0.24
[23]	1.8,2.37	1.66,1.89	42,49	3.68,3.17	0.34x0.28
[24]	9.8, 13.5	1.80,1.50	30, 23	11.9,9.8	1.22x1.22
[25]	13,14	2.86,3.37	53,33	2,1.78	3.32x1.16
[26]	3.6,6.4	1.3,1.2	31,25	8.2,6.7	0.29x0.29
[27]	5.2,5.8	2.3,1.5	22,21	2.50,1.55	0.21x0.35
[28]	7.45,10	0.83,0.95	32,31	6,4	0.50x0.75
This work	**3.45,5.4**	**0.1,0.18**	**29,32**	**4,8**	**0.28 x0.24**

IV. CONCLUTIONS

This paper presents a dual band filter with an innovative quad stub loaded UIR structure. The multipath coupling schemes (one through side stubs and another through vertical stubs) in the proposed resonator enable individual bandwidth control. In the step-by-step process of filter design, a tri mode resonator is converted into a dual mode resonator which can be finitely adjusted to provide excellent results in terms of Insertion Loss (IL) (0.10 and 0.18 dB in 1st and 2nd pass bands) and suppression of harmonic pass bands. The frequency of each resonating mode is calculated. Also, from the even-odd mode analysis the resonating conditions are derived. A methodical functional circuit diagram is presented to explain multipath coupling in terms of electrical and magnetic coupling. The simulated dual pass band filter exhibits good pass band characteristics with 3.45 and 5.4 GHz pass band center frequencies which are suitable for WiMAX and WLAN applications. Both the pass bands can be controlled individually. The stop bands characteristics are also improved with 3 TZs and by suppressing the harmonic pass bands around -20dB level. The fabricated prototype showed a great amount of correlation with simulated S_{11} and S_{21} graph.

REFERENCES

[1] J. Konpang and N. Wattikornsirikul, “Dual-mode dual-band bandpass filter with high cutoff rejection by using asymmetrical transmission zeros technique”, *Progress In Electromagnetics Research M,* vol. 100, pp. 225–236, 2021

[2] N. Wattikornsirikul and M. Kumngern, “Dual-mode dual-band bandpass filter with asymmetrical transmission zeros”, *Progress In Electromagnetics Research M,* vol. 86, pp. 193–202, 2019.

[3] Y. X. Wang, Y. L. Chen, W. H. Zou, W. -C. Yang, and J. Zen, “Dual-band bandpass filter design using stub-loaded hairpin resonator and meandering uniform impedance resonator”, *Progress In Electromagnetics Research Letters,* vol. 95, pp. 147–153, 2021.

[4] Y. -P. Zhong, Y. Xiong, and J. Huang, "Design of independently tunable dual-band filter with high selectivity and compact size using multipath propagation concept" *Progress In Electromagnetics Research Letters*, vol. 95, pp. 107–114, 2021.

[5] Z. Troudi, J. Machác and L. Osman, "Compact dual-band bandpass filter using a modified hexagonal split ring resonator", *Microw Opt Technol Lett*., vol. 62, no. 5, pp. 1893-1899, May 2020.

[6] Q. Liu, D. Zhang, J. Zhang, D. Zhou and N. An, "Compact single- and dual-band bandpass filters with controllable transmission zeros using dual-layer dual-mode loop resonators" *IET Microw. Antennas Propag.,* vol. 14, no. 6, pp. 522-531, 2020.

[7] D. Li and K. -D. Xu, "Compact dual-band bandpass filter using coupled lines and shorted stubs" *IET Elect, Lett.,* vol. 56 no. 14 pp. 721–724, Jul. 2020.

[8] D. Li, J. -A. Wang, Y. Liu, Z. Chen and L. Yang, "Selectivity-enhancement technique for parallel-coupled SIR based dual-band bandpass filter" *Microw Opt Technol Lett.,* vol. 63, no. 3, pp. 787-792, Mar. 2021.

[9] G. -Z. Liang and F. -D. Chen, "A compact dual-wideband bandpass filter based on open-/short-circuited stubs", *IEEE Access*, vol. 8, pp. 20488-20492, 2020.

[10] D. Li, J. -A. Wang, Y. Liu and Z. Chen, "Miniaturized dual-band bandpass filter with sharp roll-off using ring-loaded resonator", *IEEE Access*, vol. 8, pp. 25588-25595, 2020.

[11] X. Wang, J. Wang, L. Zhu, W. -W. Choi and W. Wu, "Compact strip line dual-band bandpass filters with controllable frequency ratio and high selectivity based on self-coupled resonator" *IEEE Trans. Microw. Theory Techn.,* vol. 68, no. 1, pp. 102–110, Jan. 2020.

[12] A. Arora, A. Madan, Sarika, M. Bhattacharjee, C. Nayak, K. V. P. Kumar and T. R. Rao, "Implementation of a compact dual-band bandpass filter using signal interference technique on paper substrate" *AEU-International Journal of Electronics and Communications,* vol. 123, pp 153-162, Aug. 2020.

[13] Zhen Tan, Qing-Yuan Lu, and Jian-Xin Chen,"Differential Dual-Band Filter Using Ground Bar-Loaded Dielectric Strip Resonators", *IEEE Microwave and Wireless Components Letters,*vol 30,Issue 2, pp 148-151,2020.

[14] Keyur Mahant and Hiren Mewada," Substrate Integrated Waveguide based dual-band bandpass filter using split ring resonator and defected ground structure for SFCW Radar applications" *Int J RF Microw Comput Aided Eng*, vol 28, issue 9,2018

[15] D. Bukuru, K. Song, F. Zhang, Y. Zhu, and M. Fan, "Compact Quad-Band Bandpass Filter Using Quad-Mode Stepped Impedance Resonator and Multiple Coupling Circuits", *IEEE Microwave and Wireless Components Letters*, vol 65, issue 3,pp 783-791 2017.

[16] Li Gao, Xiu Yin Zhang, Xiao-Lan Zhao, Yao Zhang, and Jin-Xu Xu "Novel Compact Quad-Band Bandpass Filter With Controllable Frequencies and Bandwidths" *IEEE Microwave and Wireless Components Letters,* vol 26, issue 6, 2016.

[17] M. Makimoto and S. Yamashita, "Microwave resonators and Filters for Wireless Communication", *Springer*, 2003.

[18] Changsoon Kim, Tae Hyeon Lee, Bhanu Shrestha and Kwang Chul Son "Miniaturized dual-band band pass filter based on stepped impedance resonators" *Microwave and Optical Technology Letters*,Vol. 59, No. 5, pp 1116-1119, 2017.

[19] Zhongbao Wang, Zheng Fu, Chengze Li, Shaojun Fang, and Hongmei Liu," A Compact Negative-Group-Delay Microstrip Bandpass Filter", *Progress In Electromagnetics Research Letters,* Vol. 90, pp 45–51, 2020.

[20] Te Shao, Zhongbao Wang, Shaojun Fang, Hongmei Liu, and Zhi Ning Chen, "A Full-Passband Linear-Phase Band-Pass Filter Equalized With Negative Group Delay Circuits" *IEEE Access*, Vol 8, 2020.

[21] Jing-Ya Deng, Chong-Hao Tan, Si-Min Hou, Dong-Quan Sun and Li-Xin Guo," A compact dual-band filtering antenna for wireless local area network applications", *Int J RF Microw Comput Aided Eng*, vol29, issue 9, 2019.

[22] Min-Hang Weng, Chun-Yueh Huang, Shi-Wei Dai and Ru-Yuan Yang," An Improved Stop band Dual-Band Filter Using Quad-Mode Stub-Loaded Resonators" *Special Issue Microwave Devices Design and Application, Electronics*,2021.

[23] Amir Nosrati, Mahmud Mohammad-Taheri and Mehdi Nosrati," Dual-to-quad-band evanescent-mode substrate-integrated waveguide band-pass filters", *IET Microw. Antennas Propag*, Vol. 14 Issue. 11, pp 1229-1240, 2020.

[24] Ling-Feng Shi, Chen-Yang Sun1, Sen Chen1, Gong-Xu Liu1 and Yi-Fan Shi," Dual-band substrate integrated waveguide bandpass filter based on CSRRs and multimode resonator". *Int J RF Microw Comput Aided Eng*, vol 28, issue 9, 2018.

[25] Hao-Wei Xie, Kang Zhou, Chun-Xia Zhou and Wen Wu "Compact wide-stop band SIW dual-band filter with closely spaced passbands", E*lectronics* Letters Vol. 56 No. 16 pp. 822–825, 2020.

[26] Hao Zhang, Wei Kang, and Wen Wu "Miniaturized Dual-Band SIW Filters Using E-Shaped Slot lines With Controllable Center Frequencies", *IEEE Microwave and Wireless Components Letters,* Volume: 28, Issue: 4, pp 311-313, 2018.

[27] Ashraf Y. Hassan and Mahmoud A. Abdalla "A Double Optimized Transmission Zeros Based on π-CRLH Dual-Band Bandpass Filter", *Progress In Electromagnetics Research Letters,* Vol. 84, pp 131–137, 2019.

[28] Sheng Zhang, Jia-Yu Rao, Jia-Sheng Hong and Fa-Lin Liu "A Novel Dual-Band Controllable Bandpass Filter Based on Fan-Shaped Substrate Integrated Waveguide", *IEEE Microwave and Wireless Components Letters,* vol 18, issue 4, 2018.